



**HAL**  
open science

## Use of epitaxial PZT thin films for $\text{La}_{2/3}\text{Sr}_{1/3}\text{MnO}_3$ based MEMs devices on $\text{SrTiO}_3/\text{Si}$

Laryssa Carvalho de Araujo, J J Manguеле, Bertrand Vilquin, Zhe Wang, Carolina Adamo, Pedro Rojo Romeo, Christophe Cibert, Gilles Poullain, Bernadette Domengès, Victor Pierron, et al.

### ► To cite this version:

Laryssa Carvalho de Araujo, J J Manguеле, Bertrand Vilquin, Zhe Wang, Carolina Adamo, et al.. Use of epitaxial PZT thin films for  $\text{La}_{2/3}\text{Sr}_{1/3}\text{MnO}_3$  based MEMs devices on  $\text{SrTiO}_3/\text{Si}$ . DTIP'2021 (23rd edition of the Symposium on Design, Test, Integration & Packaging of MEMS and MOEMS), Aug 2021, ONLINE - Lyon, France. pp.01-05, 10.1109/DTIP54218.2021.9568662 . hal-03431593

**HAL Id: hal-03431593**

**<https://hal.science/hal-03431593>**

Submitted on 8 Nov 2022

**HAL** is a multi-disciplinary open access archive for the deposit and dissemination of scientific research documents, whether they are published or not. The documents may come from teaching and research institutions in France or abroad, or from public or private research centers.

L'archive ouverte pluridisciplinaire **HAL**, est destinée au dépôt et à la diffusion de documents scientifiques de niveau recherche, publiés ou non, émanant des établissements d'enseignement et de recherche français ou étrangers, des laboratoires publics ou privés.

# Use of epitaxial PZT thin films for $\text{La}_{2/3}\text{Sr}_{1/3}\text{MnO}_3$ based MEMS devices on $\text{SrTiO}_3/\text{Si}$

Laryssa Mirelly Carvalho de Araujo  
Normandie Univ, UNICAEN,  
ENSICAEN, CNRS, GREYC  
Caen, France  
laryssa.carvalho-dearaujo@unicaen.fr

Jacques Junior Manguelle  
Normandie Univ, UNICAEN,  
ENSICAEN, CNRS, CRISMAT  
Caen, France  
jacques-junior.manguelle@ensicaen.fr

Bertrand Vilquin  
Université de Lyon, Ecole centrale de  
Lyon, INL UMR CNRS 5270  
Ecully, France  
bertrand.vilquin@ec-lyon.fr

Zhe Wang  
Department of Materials Science and  
Engineering, Cornell University,  
Ithaca, New York, USA  
100wang001zhe@163.com

Carolina Adamo  
Department of Materials Science and  
Engineering, Cornell University,  
Ithaca, New York, USA  
carolinaadamo30@gmail.com

Pedro Rojo Romeo  
Université de Lyon, Ecole centrale de  
Lyon, INL UMR CNRS 5270  
Ecully, France  
pedro.rojo-romeo@ec-lyon.fr

Christophe Cibert  
Normandie Univ, UNICAEN,  
ENSICAEN, CNRS, CRISMAT  
Caen, France  
christophe.cibert@ensicaen.fr

Gilles Poullain  
Normandie Univ, UNICAEN,  
ENSICAEN, CNRS, CRISMAT  
Caen, France  
gilles.poullain@ensicaen.fr

Bernadette Domengès  
Normandie Univ, UNICAEN,  
ENSICAEN, CNRS, CRISMAT  
Caen, France  
bernadette.domenges@ensicaen.fr

Victor Pierron  
Normandie Univ, UNICAEN,  
ENSICAEN, CNRS, GREYC  
Caen, France  
victor.pierron@ensicaen.fr

Darrell G. Schlom  
Department of Materials Science and  
Engineering, Cornell University  
& Kavli Institute at Cornell for  
Nanoscale Science, Cornell University  
Ithaca, New York, USA  
schlom@cornell.edu

Laurence Méchin  
Normandie Univ, UNICAEN,  
ENSICAEN, CNRS, GREYC  
Caen, France  
laurence.mechin@ensicaen.fr

**Abstract**—Lead zirconate titanate  $\text{Pb}(\text{Zr},\text{Ti})\text{O}_3$  (PZT) is a well known ferroelectric material with excellent piezoelectric properties, namely large piezoelectric coefficients, low leakage current and reliable performance, which makes it very suitable as an actuator material in Micro-ElectroMechanical Systems (MEMS). The performance of piezoelectric MEMS is, however, strongly dependent on the film quality. In the present work, the epitaxial growth of PZT is desired as it can help to reduce high-frequency losses, to allow for larger electromechanical coupling and to increase the final device sensitivity. We used an epitaxially grown conductive oxide bottom electrode, namely 45 nm thick  $\text{La}_{2/3}\text{Sr}_{1/3}\text{MnO}_3$  (LSMO) films, deposited on  $\text{SrTiO}_3$  buffered (001) silicon substrates using a combination of pulsed laser deposition and reactive molecular beam epitaxy techniques. The 500 nm thick c-axis oriented PZT layers were deposited at 600°C by magnetron sputtering on the LSMO films on  $\text{STO}/\text{Si}$  (001). The piezoelectric and ferroelectric properties of the PZT layers were studied by PiezoForce Microscopy on as-grown PZT films and Polarization versus Electric field measurements on samples covered with Pt top electrodes. The PZT films exhibited good piezoelectric and ferroelectric properties with a remanent polarization higher than  $20 \mu\text{C}\cdot\text{cm}^{-2}$ , which makes them suitable for the fabrication of piezoelectric MEMS based on doubly-clamped LSMO suspended structures.

**Keywords**—Epitaxial PZT; piezoelectric MEMS; Oxide electrodes; PFM

## I. INTRODUCTION

Micro-ElectroMechanical systems (MEMS) are micrometer devices with movable parts fabricated through microtechnology tools and are widely used in various sensors

and actuators applications.  $\text{La}_{2/3}\text{Sr}_{1/3}\text{MnO}_3$  (LSMO) presents a ferromagnetic-to-paramagnetic transition at about 360 K that is accompanied by a metal-to-insulator transition above room temperature, which is very promising for uncooled sensors, such as anisotropic magnetoresistances [1] or infrared bolometers [2]. In addition, the high sensitivity of epitaxial oxides to strain, hence to mechanical effects, makes these materials promising and encourage us to investigate the potentialities of LSMO based MEMS resonators [3].

The objective of the present paper is to demonstrate the integration of c-axis oriented  $\text{Pb}(\text{Zr},\text{Ti})\text{O}_3$  (PZT) thin films on LSMO/ $\text{SrTiO}_3$ (STO)/Si free-standing doubly-clamped structures. Epitaxial growth of PZT is required in order to allow lower voltage actuation and higher sensitivity detection, through inverse and direct piezoelectric effects, due to the larger electro-mechanical coupling than those obtained with polycrystalline films [4]. Besides epitaxy, the integration of PZT on a conductive oxide electrode is expected to provide better fatigue performances and suppression of dead-layers in the PZT film [5][6][7], leading to long-lasting final devices. During polarization cycles, the interface between PZT and LSMO, with its characteristic of a wide bandgap p-type semiconductor, is free of charge accumulation, such that, with no carrier injection leading to accumulation of  $\text{O}_2$  vacancies [8][9], the fatigue problems are expected to be further minimized [10][11].

After a brief description of the experimental methods in section II, we will present the structural and morphological properties of the deposited layers in section III and the electrical properties in section IV. Conclusions are given in section V.

## II. EXPERIMENTAL METHODS

### A. Thin film deposition

The PZT/LSMO/STO/Si heterostructures were obtained thanks to the successive use of 3 different deposition methods. First 20 nm thick STO layers were deposited by molecular-beam epitaxy on 3-inch (001) silicon wafers following the same process as reported previously [12]. STO covered Si wafers were cut into  $10 \times 10 \text{ mm}^2$  squares and about 2 nm thick STO followed by 45 nm thick LSMO films were deposited by pulsed laser deposition at  $750^\circ\text{C}$  and 20 Pa of  $\text{O}_2$ .

We selected the chemical composition  $\text{Zr}:\text{Ti}=52:48$  of PZT, since it exhibits the material's largest piezoelectric coefficient, near the so called morphotropic phase boundary. 500 nm thick PZT thin films were deposited on the LSMO/STO/Si samples in a multi-target RF magnetron sputtering system from 3 metallic targets using power during deposition of  $\text{Pb} : 0.7 \text{ W}\cdot\text{cm}^{-2} / \text{Zr} : 2.7 \text{ W}\cdot\text{cm}^{-2} / \text{Ti} : 3.3 \text{ W}\cdot\text{cm}^{-2}$ , in a pressure of 0.7 Pa of 90% Ar / 10%  $\text{O}_2$  atmosphere at  $600^\circ\text{C}$ .

### B. Characterization methods

The crystallinity of the samples was characterized by performing X-ray diffraction (XRD) measurements in  $\theta$ - $2\theta$  configuration as well as rocking curves around the 002 peak of PZT, where the full-width at half-maximum (FWHM) of the peak could be estimated. The data were collected using a PANalytical X'Pert PRO diffractometer with  $\text{Cu-K}\alpha$  radiation.

Atomic Force Microscopy (AFM) measurements using a Nano-Observer system from Concept Scientific Instruments were performed to characterize the surface morphology of the films in resonant mode with standard Al-coated Si probes showing nominal resonant frequency of 300 kHz. In addition Piezoresponse Force Microscopy (PFM) employing doped diamond probes with an elastic constant of about  $2.8 \text{ N}\cdot\text{m}^{-1}$  was used to investigate the piezoelectric properties of the as-grown PZT films on LSMO/STO/Si (001).

Pt layers were finally deposited on the PZT films by sputtering at room temperature and patterned using a lift-off process in order to design top electrodes of  $250 \times 250 \mu\text{m}^2$  size and to perform polarization hysteresis ( $P - E$ ) loop measurements using a Sawyer-Tower (ST) circuit, driven by a sine wave of amplitude 20 V and frequency 500 kHz. The capacitors were contacted on a Suss MicroTec PM5 probe station. A standard capacitor  $C_{\text{st}}$  of 22 pF serving as a charge holder, was used during the hysteresis measurements.

### III. STRUCTURAL AND MORPHOLOGICAL PROPERTIES

The epitaxial growth of LSMO and PZT on STO/Si was confirmed by XRD, as shown in the  $\theta$ - $2\theta$  scan of Fig. 1, where the  $00l$  peaks of the aforementioned layers were observed. No parasitic phases of the PZT were observed. The FWHM of the rocking curve around the 002 peak of PZT presented in Fig. 2 was equal to  $0.35^\circ$ , confirming the high structural quality of the deposited layers.

The  $2 \times 2 \mu\text{m}^2$  AFM images of LSMO and PZT layers are presented in Fig. 3. Both LSMO and PZT showed smooth surfaces. LSMO and PZT rms roughness was equal to  $0.3 \pm 0.04 \text{ nm}$  and  $1 \pm 0.1 \text{ nm}$ , respectively.

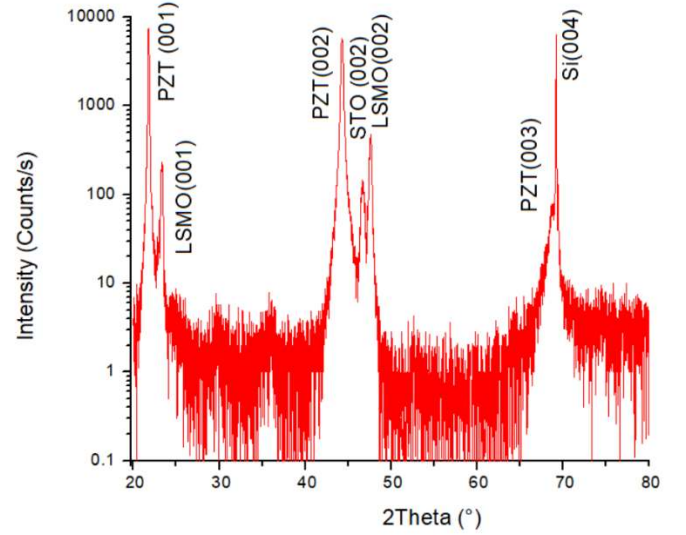


Fig. 1. X-Ray Diffraction  $\theta$ - $2\theta$  scan of epitaxial PZT/LSMO/STO/Si heterostructure showing the  $00l$  peaks of all layers.

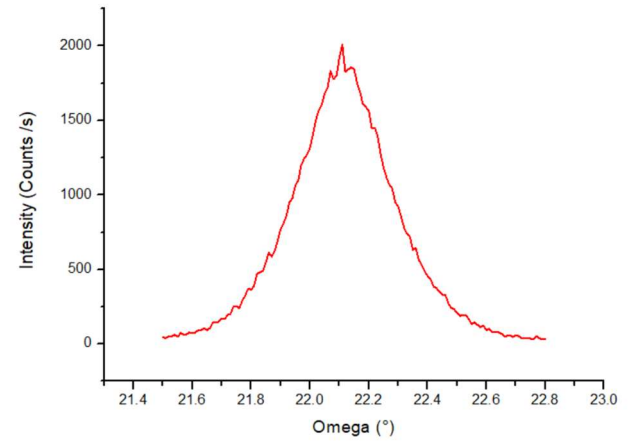
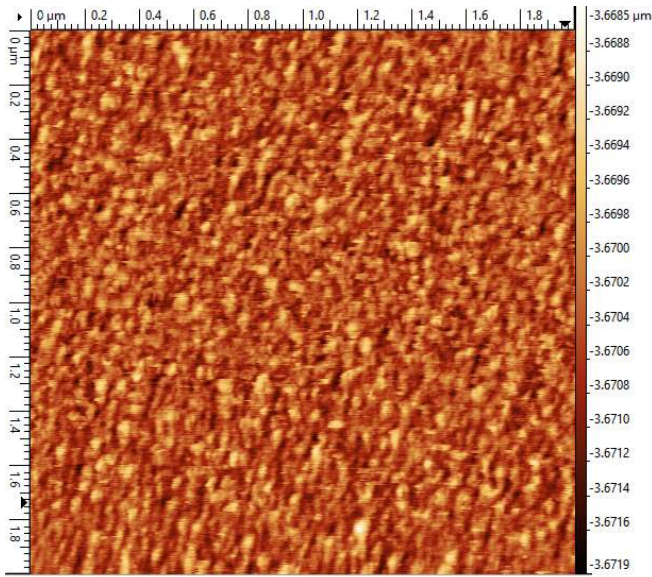


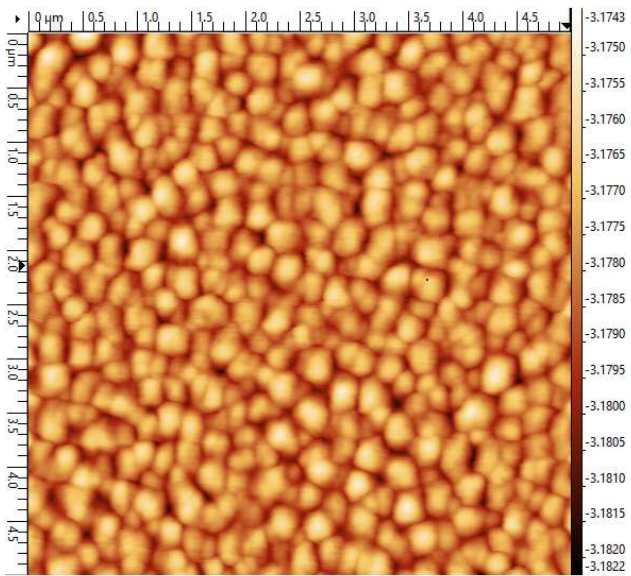
Fig. 2. Rocking curve ( $\omega$ -scan) around the 002 peak of PZT showing a FWHM of  $0.35^\circ$ .

## IV. ELECTRICAL PROPERTIES

The piezoelectric and ferroelectric properties were first characterized by PFM measurements through the creation of artificial domains by poling a  $5 \times 5 \mu\text{m}^2$  surface through a scanning with +10V dc voltage applied on the cantilever tip (domain down), followed by -10V dc voltage to reverse the piezoelectric dipoles in a  $2 \times 2 \mu\text{m}^2$  surface central area (domain up). The out-of-plane piezoelectric response was then collected with a 4 V ac drive voltage at 330 kHz in a  $15 \times 15 \mu\text{m}^2$  scan. As exhibited in Fig. 4, the poling was uniformly and completely achieved. The two stable states of polarization were maintained showing good ferroelectric properties of the deposited PZT film at low voltage compatible with a final MEMS device actuation.



(a)



(b)

Fig. 3. AFM images of (a)  $2 \times 2 \mu\text{m}^2$  scan of the 45 nm thick LSMO layer on STO/Si (001) and (b)  $5 \times 5 \mu\text{m}^2$  scan of the 500 nm thick PZT layer on LSMO/STO/Si (001).

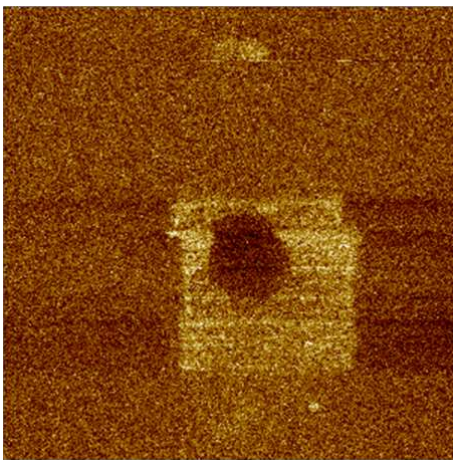


Fig. 4.  $15 \times 15 \mu\text{m}^2$  phase image in PFM mode for a 500 nm thick PZT film deposited by sputtering at  $600^\circ\text{C}$ . Squares of  $2 \times 2 \mu\text{m}^2$  and  $5 \times 5 \mu\text{m}^2$  size were first written with -10 V and +10 V tip voltage, respectively.

Spectroscopy measurements during which the area underneath the PFM tip is switched between -10 V and +10 V and back were performed inside the previously polarized area in order to acquire series of hysteresis loops using the same tip as used for imaging. The displacement versus applied voltage was measured with a drive voltage of 5 V and is displayed in Fig. 5. We could observe the typical butterfly-shaped curves measured in piezoelectric materials showing ferroelectric switching effect.

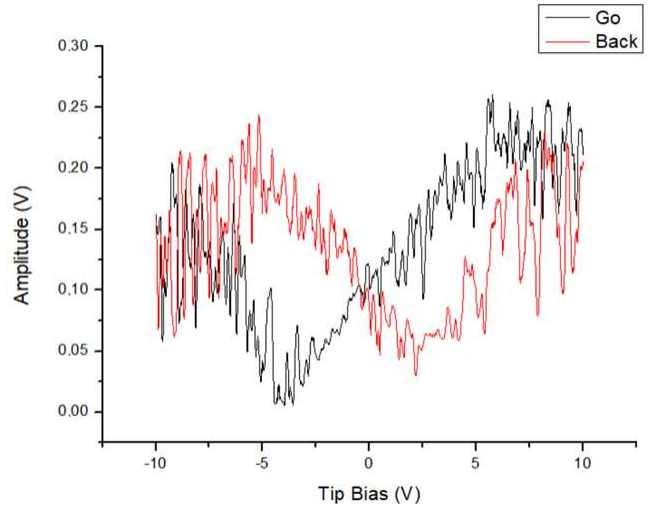


Fig. 5. The typical displacement versus tip voltage curve measured with a drive voltage of 5 V

The macroscopic polarization hysteresis curves,  $P(E)$ , of the PZT films were performed on samples with top Pt electrodes. A decentralized cycle in the x axis was observed due to the different top and bottom electrode materials, being Pt and LSMO, respectively. The cycle exhibited a low coercive field and remanent polarization of about  $22 \mu\text{C}\cdot\text{cm}^{-2}$ , in accordance with typical values found in the literature [13] indicating excellent ferroelectric properties.

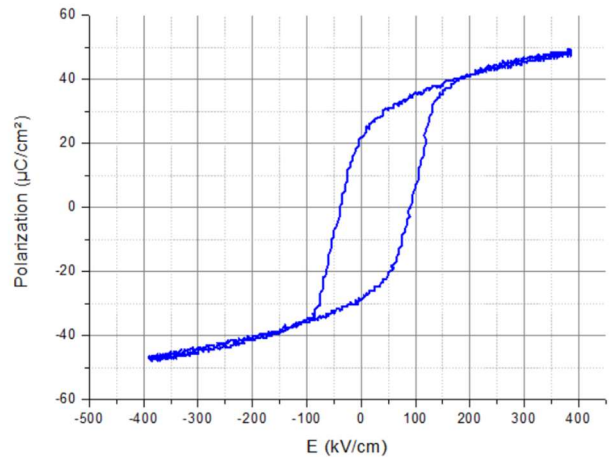


Fig. 6. Polarization versus electric field hysteresis loop measured with bottom LSMO electrodes and top Pt electrodes.

## V. CONCLUSIONS

The successful integration of *c*-axis PZT deposited by magnetron sputtering at  $600^\circ\text{C}$  on LSMO/STO/Si was confirmed by XRD showing the 00 $l$  peaks of the PZT layer, as well as those of LSMO and STO with FWHM of the rocking curve around the 002 peak of PZT equal to  $0.35^\circ$ .

The artificial domains created by PFM were stable for several hours. The PFM displacement versus tip voltage curves showed the typical butterfly-shaped curves measured in piezoelectric materials showing ferroelectric switching effect and P(E) curves have exhibited good electrical properties, overall showing that these PZT thin films can be used for MEMS actuation.

These PZT layers will now be integrated in suspended LSMO bridges using a combination of ion beam etching in argon and reactive ion etching in SF<sub>6</sub> gas using a fabrication process adapted from [14].

#### ACKNOWLEDGMENTS

L.M.C.A. was supported by a PhD grant RIN Doctorants 100% from Région Normandie.

#### REFERENCES

- [1] L.G. Enger, S. Flament, I.-N. Bhatti, B. Guillet, M. Lam Chok Sing, O. Rousseau, V. Pierron, S. Lebagry, J.-M. Diez, A. Vera, I. Martinez, R. Guerrero, L. Perez, P. Perna, J. Camarero, R. Miranda, M.T. Gonzalez, L. Méchin, "Sub-nT resolution of Single Layer Sensor Based on the AMR Effect in La<sub>2/3</sub>Sr<sub>1/3</sub>MnO<sub>3</sub> Thin Films" in IEEE Transactions on Magnetics, doi: 10.1109/TMAG.2021.3089373.
- [2] V. M. Nascimento, L Méchin, S. Liu, A. Aryan, C. Adamo, D. G. Schlom, B. Guillet, "Electro-thermal and optical characterization of an uncooled suspended bolometer based on an epitaxial La<sub>0.7</sub>Sr<sub>0.3</sub>MnO<sub>3</sub> film grown on CaTiO<sub>3</sub>/Si", J. Phys. D: Appl. Phys. vol. 54 055301, 2021.
- [3] D.T. Huong Giang, N.H. Duc, G. Agnus, T. Maroutian, P. Lecoeur, "Fabrication and characterization of PZT string based MEMS devices", Journal of Science: Advanced Materials and Devices, vol. 1, pp. 241-219, 2016.
- [4] S. Yin, G. Niu, B.Vilquin, B.Gautier, G.Le Rhun E.Defay Y.Robach, "Epitaxial growth and electrical measurement of single crystalline Pb(Zr<sub>0.52</sub>Ti<sub>0.48</sub>)O<sub>3</sub> thin film on Si(001) for micro-electromechanical systems", Thin Solid Films, vol. 250, pp. 4572-4575, 2012.
- [5] R. Ramesh, W.K. Chan, B. Wilkens, H. Gilchrist, T. Sands, J.M. Tarascon, D.K. Fork, J.Lee, A. Safari, "Fatigue and retention in ferroelectric Y-Ba-Cu-O/Pb-Zr-Ti-O/Y-Ba-Cu-O heterostructures", Applied Physics Letters, vol. 61, no. 1537, 1992
- [6] C. B. Eom, R. B. Van Dover, J. M. Phillips, D. J. Werder, J. H. Marshall, C. H. Chen, R. J. Cava, R. M. Fleming, and D. K. Fork, "Fabrication and properties of epitaxial ferroelectric heterostructures with (SrRuO<sub>3</sub>) isotropic metallic oxide electrodes", Applied Physics Letters, vol. 63, no. 2570, 1993
- [7] N. Sama, R. Herdier, D. Jenkins, C. Soyer, D. Remiens, R. Bouregba, "On the Influence of the Top and Bottom Electrodes—A Comparative Study between Pt and LNO Electrodes for PZT Thin Films", J. Cryst. Growth 310, 3299, 2008.
- [8] Seshu B. Desu, "Influence of stresses on the properties of the ferroelectric BaTiO<sub>3</sub> thin films", Journal of the electromechanical Society, vol. 140, no. 10, 1993
- [9] D. J. Wouters, G. Willems, G. Groeseneken, H. E. Maes, K. Brooks, "Elements of the leakage current of high ε ferroelectric PZT films", Integrated Ferroelectrics, vol. 7, no. 1-4, 1995
- [10] P. M. Leufke, D. Wang, R. Kruk, C. Kübel, "Ferroelectric vs. structural properties of large-distance sputtered epitaxial LSMO/PZT heterostructures", vol. 2, no. 032184, 2012
- [11] H. Funakubo, M. Dekkers, A. Sambri, S. Gariglio, I. Shklyarevskiy, G. Rijnders, "Epitaxial PZT films for MEMS printing applications", Mrs Bulletin, vol. 37, 2012.
- [12] M. P. Warusawithana, C. Cen, C. R. Slesman, J. C. Woicik, Y. Li, L. F. Kourkoutis, J. A. Klug, H. Li, P. Ryan, L.-P. Wang, M. Bedzyk, D. A. Muller, L.-Q. Chen, J. Levy, and D. G. Schlom, Science 324, 367, 2009.

- [13] R. Bouregba, B. Vilquin, G. Le Rhun, G. Poullain, B. Domenges, "Sawyer-Tower hysteresis measurements on micron sized Pb(Zr,Ti)O<sub>3</sub> capacitors", Review of Scientific Instruments, vol. 74, 10, 2003.
- [14] S. Liu, B. Guillet, C. Adamo, V.M. Nascimento, S. Lebagry, G. Brasse, F. Lemarié, J. Elfallah, D.G. Schlom, L. Mechin, "Free-standing La<sub>0.7</sub>Sr<sub>0.3</sub>MnO<sub>3</sub> suspended micro-bridges on buffered silicon substrates showing undegraded low frequency noise properties", J. Micromech. Microeng., vol. 29, 065008, 2019.

